



Silica-tethered cuprous acetophenone thiosemicarbazone (STCATSC) as a novel hybrid nano-catalyst for highly efficient synthesis of new 1,2,3-triazolyl-based metronidazole hybrid analogues having potent anti-giardial activity

Mohammad Navid Soltani Rad¹ | Somayeh Behrouz¹ | Javad Mohammadtaghi-Nezhad¹ | Elham Zarenezhad² | Mahmoud Agholi²

¹ Medicinal Chemistry Research Laboratory, Department of Chemistry, Shiraz University of Technology, Shiraz 71555-313, Iran

² Noncommunicable Diseases Research Center, School of Medicine, Fasa University of Medical Sciences, Fasa, Iran

Correspondence

Mohammad Navid Soltani Rad and Somayeh Behrouz, Medicinal Chemistry Research Laboratory, Department of Chemistry, Shiraz University of Technology, Shiraz 71555-313, Iran.
Email: soltani@sutech.ac.ir; behrouz@sutech.ac.ir

The preparation, characterization and application of silica-tethered cuprous acetophenone thiosemicarbazone (STCATSC) as a novel hybrid nano catalyst for synthesis of new 1,2,3-triazolyl-based metronidazole hybrid analogues is described. STCATSC is fully characterized by different microscopic, spectroscopic and physical techniques, including scanning electron microscopy (SEM), transmission, X-ray diffraction (XRD), Energy-dispersive X-ray spectroscopy (EDS), thermogravimetric analysis (TGA), FT-IR and inductively coupled plasma (ICP) analysis. This catalyst is used to prepare the new 1,2,3-triazolyl-based metronidazole hybrid analogues. The 'Click' Huisgen cycloaddition reaction of 2-methyl-5-nitro-1-prop-2-ynyl-1H-imidazole with diverse β -azidoalcohols in a THF-water media at R.T. provides the products in good to excellent yields using STCATSC. STCATSC is proved to be a stable, low cost, reusable and environmentally benign hybrid catalyst. Products are *in vitro* tested against *Giardia lamblia* (*G. lamblia*) in which determined that all compounds exhibit varied promising anti-giardial activity compare to metronidazole as a reference drug. Among the products, 1-(4-((2-methyl-5-nitro-1H-imidazol-1-yl)methyl)-1H-1,2,3-triazol-1-yl)-3-phenethoxypropan-2-ol and 1-(4-((2-methyl-5-nitro-1H-imidazol-1-yl)methyl)-1H-1,2,3-triazol-1-yl)-3-(3-phenylpropoxy)propan-2-ol are demonstrated to exhibit the potent anti-giardial activity even stronger than metronidazole.

KEYWORDS

1,2,3-triazolyl-based metronidazole hybrid analogue, 2-methyl-5-nitro-1-prop-2-ynyl-1H-imidazole, *Giardia lamblia*, STCATSC, β -Azidoalcohol

1 | INTRODUCTION

There is no doubt that among known bioactive *N*-Heterocyclic compounds, nitroimidazole (NIM) cores

exhibit brilliant and remarkable pharmaceutical activities.^[1] Since the discovery of an antiparasitic azomycine **1** in the 1950s from *Streptomyces* bacteria,^[2] further explorations has inspired the invention of metronidazole

2 (MTZ) as the prototype for the NIM-class of antimicrobials and the subsequent emergence of next generations of NIM-drugs **3–11** (Figure 1).^[3]

NIM derivatives are well-established chemotherapeutic agents with broad spectrum activity against parasites involving anaerobic protozoa, mycobacteria, anaerobic bacteria, gram-positive and gram-negative bacteria, fungal and HIV.^[4] The versatility of NIM drugs has emerged them as drugs of choice against multifarious infections caused by neglected tropical diseases (NTD),^[5] in particular human African trypanosomiasis (HAT), chagas disease, leishmaniasis, tuberculosis (TB) and malaria.^[6] In addition NIM-drugs extensively are applied to inhibit *Trichomonas vaginalis*,^[7] *Entamoeba histolytica*, *Giardia lamblia* and *Helicobacter pylori*.^[8] NIM-drugs have found the utility as radiosensitizing agents in cancer treatment,^[9] and also exploited in tumour hypoxia imaging for cancer management.^[10] Although the presence of toxicophoric nitro moiety in drugs' scaffolds is undesirable due to its potential hepatotoxicity and mutagenicity,^[11] however the nitro group in NIMs exhibits a crucial role for its antiinfective activity.^[12] As matter of fact, the NIM cores in drugs **1–11** and also other NIM derivatives are known as a warhead where the nitro group has the ignition source or trigger role.^[13] This property is owing to the fact that the nitro moiety is reduced to reactive radical species under enzymatic reaction by diverse reducing enzymes such as ferredoxin and/or thioredoxin reductase (TrxR) found in pathogenic microorganisms.^[14] This reactive radical species then attack to DNA which result in devastating of microorganism. Despite the significance of NIM-drugs in fight against pathogenic microbes, however NIM-resistance as well as toxicity was observed for some NIM-drugs. As instance, MTZ-resistance in *Giardia Lamblia* and *Trichomonas vaginalis* have been well-documented.^[15] Thus, in this connection the design and synthesis of new NIM-drugs to overcome these drawbacks is critically essential. Keeping the NIM core intact, one-way to acquire the new derivatives is variation in *N*-alkyl residue.^[16] The change

in NIM substituents is an attractive strategy since it leads to different spectra of activity and pharmacokinetic profiles. Additionally, changes in *N*-alkyl residue of NIMs affects the redox potential of the electron-transport in nitro group and thus alters the cytotoxicity.

The merging of the 1*H*-1,2,3-triazolyl core into a molecular framework is an interesting strategy for enhancing the chance of biological activity owing to its well recognition by target proteins in the cell. Moreover, 1*H*-1,2,3-triazolyl group are known as the non-classical bioisostere of amide since their extensive similarity in size, polarity, hydrogen bonding, and dipole moment. They have also been applied as a linker or spacer to conjunct two pharmacophores in a drug's scaffold.^[17] In this context, MTZ-triazole conjugates have recently reported by several research teams. Negi and coworkers have shown that the hydroxyl group of MTZ is amenable to modification.^[18,19] They have replaced the hydroxyl with 1,2,3-triazolyl moiety utilizing a modular synthesis through the copper(I)-catalyzed azide-alkyne cycloaddition (CuAAC). The MTZ-triazole hybrids **12** demonstrated the potent to weak antibacterial activity against Gram-positive and Gram-negative bacteria (Figure 2). Independently, Miyamoto et al. reported a similar approach to Mtz-triazole hybrids **12** and also other hybrid analogues **13** which were prepared by reaction of different 5-nitroimidazole azides with a library of alkynes.^[20] They observed that some Mtz-triazole hybrids exhibit the improved activity against a range of microbes such as *Giardia lamblia*, *Trichomonas vaginalis*, *Helicobacter pylori*, *Clostridium difficile*, and *Bacteroides fragilis*. Jarrad et al. also extended the synthesis of a library of structurally related MTZ-triazole hybrids **12**.^[21] Several compounds were determined with excellent broad spectrum activity targeting *Clostridium difficile*, *Entamoeba histolytica*, and *Giardia lamblia*.

Grafting of the organic molecules onto the solid inorganic surfaces is an appealing route to access organic-inorganic hybrid catalysts (OIHCs).^[22] In recent years, OIHCs has found increasing attention in organic

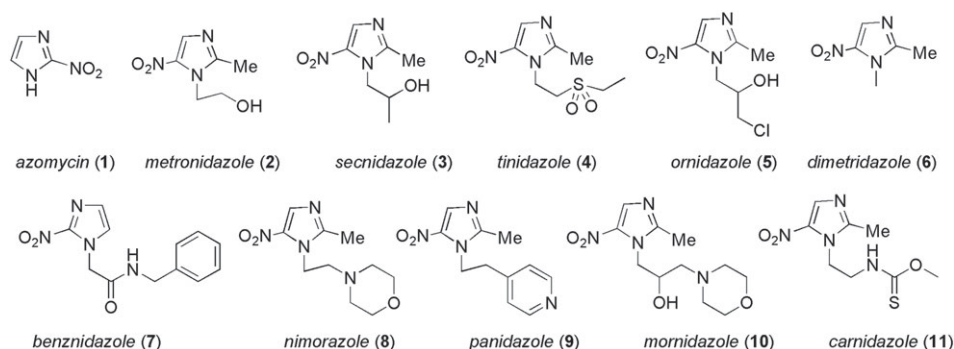


FIGURE 1 The structure of well-known NIM-drugs

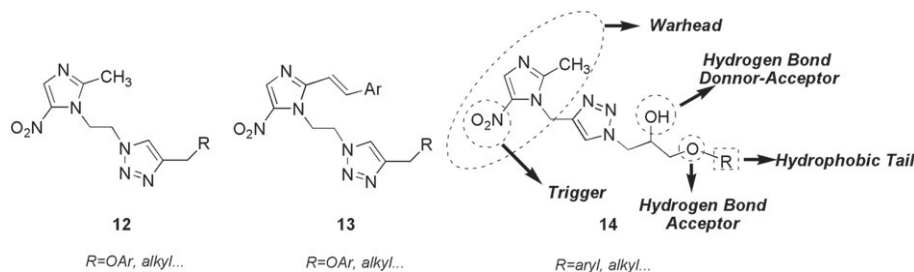


FIGURE 2 The structure of MTZ-triazole hybrids (**12** and **13**) and our new 1,2,3-triazolyl-based MTZ hybrid analogues (**14**)

synthesis owing to their heterogeneous nature and extensive advantages such as the separation simplicity, ease of handling, cheapness, high selectivity, chemical and thermal stabilities.^[23] Among OIHCs, silica-based OIHCs are interesting since silica is abundantly available and exhibits high stability.^[24] In addition, the amorphous, mesoporous, and zeolitic silica materials can be covalently tethered to diverse organic moieties to provide the proper sites for chelation with active metal ions.^[25] In this connection, active Cu^{I} species has widely applied in OIHCs structure due to the importance of Cu^{I} catalytic property in many organic transformations particularly in Huisgen Cu^{I} -catalyzed azide-alkyne cycloaddition (CuAAC).^[26] As the catalytic species, an active Cu^{I} displays a crucial role in the regioselectivity of the 'Click' Huisgen cycloaddition, merely providing 1,4-disubstituted isomers. However, the use of Cu^{I} salts in traditional form was limited since the formation of unwanted side products like alkyne-alkyne

homocoupling adducts.^[27] To dispel this problem, Cu^{I} is mostly linked to N- or P-based free ligands and/or supported ligands onto the surface of diverse solids.^[28] This chelation improves the Cu^{I} -catalytic activity and thus prevents desorption of Cu species from the surface of the catalyst which enhances the reusability.^[29]

In pursuit of our ongoing research on preparation of copper heterogeneous nano-catalysts and their application in numerous organic transformations^[30–32] hereby, we would like to report the synthesis and characterization of silica-tethered cuprous acetophenone thiosemicarbazone (STCATSC) as a novel hybrid nano-catalyst (Figure 3) and applied this nano-hybrid catalyst in synthesis of new 1,2,3-triazolyl-based metronidazole hybrid analogues **14**. In addition, we assessed the *in vitro* antiparasitic screening of compounds **14** against *Giardia lamblia*.

2 | RESULTS AND DISCUSSION

2.1 | Preparation of STCATSC

The process for the preparation of STCATSC is shown in Scheme 1. As indicated, the synthesis of STCATSC is started from traditional SiO_2 . For the optimal reaction of SiO_2 , it was first activated by a flow of 8% O_2 in an argon atmosphere for 1 hr in a furnace at 400 °C. Activation of SiO_2 using O_2 at high temperature, provides further hydroxyl moieties at the surface of silica structure.^[33] Then, the activated SiO_2 (**I**) which formerly was

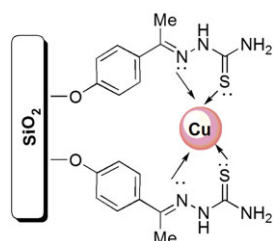
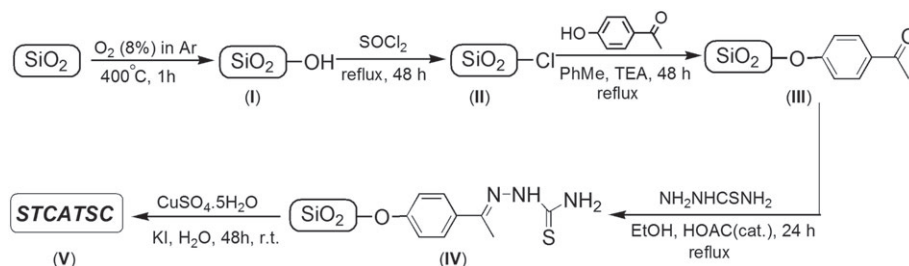


FIGURE 3 The structure of silica-tethered cuprous acetophenone thiosemicarbazone (STCATSC) as a novel hybrid nano-catalyst



SCHEME 1 Preparation of silica-tethered cuprous acetophenone thiosemicarbazone (STCATSC)

anhydrous in a vacuum oven at 250 °C, converted to silica chloride (II) via thionyl chloride due to the standard procedure described in a literature.^[34] Afterward, to a solution containing 4-hydroxyacetophenone and trimethylamine in anhydrous toluene, it was gradually added the silica chloride during half of an hour at ambient temperature and subsequently was refluxed for 48 hr. The suspension was filtered and the remaining solid (III) was washed with anhydrous toluene and kept in a vacuum oven at 50 °C for a night. The obtained creamy powder (III) was then suspended in a solution containing thiosemicarbazide and a few drops of HOAc in ethanol which refluxed for a day. The filtration of suspension mixture followed by washing the remaining residue by ethanol acquired a yellowish solid (IV) which kept in a vacuum oven at 50 °C for few hours (6 hr). Then, the acquired solid (IV) was immersed and vigorously stirred in a solution of $\text{CuSO}_4 \cdot 5\text{H}_2\text{O}$ and KI in distilled water at R.T. for two days. Afterward of separation of solid (filtration) and washing with plenty of distilled water, the obtained grey solid (V) was dried in a vacuum oven at 100 °C for few hours and finally stored in a desiccator (Figure 4).

2.2 | Characterization of catalyst

The powder X-ray diffraction pattern of the STCATSC obtained by precipitation from freshly prepared aqueous STCATSC suspension at 10–90 °C (Figure 5). Regarding to XRD pattern, the courier peak at $2\theta = 25.678^\circ$ is related to the presence of SiO_2 in the catalyst structure (Table 1). In addition, the angles of $2\theta = 42.472^\circ$ and $2\theta = 50.189^\circ$ represents the copper nano particles in the catalyst. Other particles matrixes and morphologies are depicted in Table 1. The crystalline size is calculated from

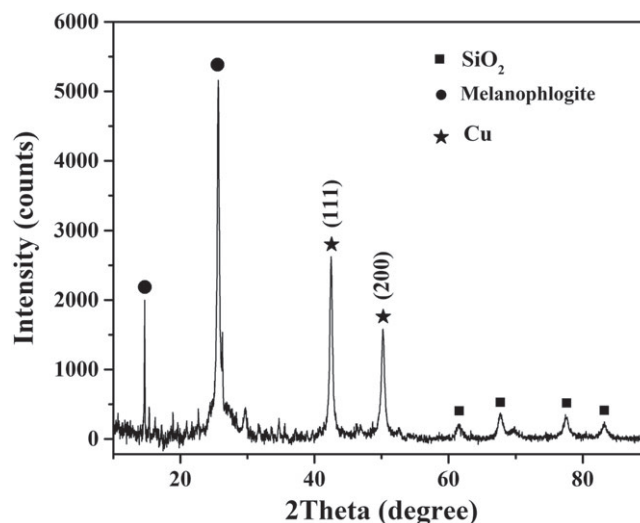


FIGURE 5 XRD Pattern of the STCATSC

TABLE 1 Analysis of XRD patterns related to STCATSC

2-Theta-scale (2 θ)	Matrix and Morphology	Reference Pattern
14.581	●	00-016-0331
25.678	●	00-016-0331
42.472	(111)★	00-004-0836
50.189	(200)★	00-004-0836
61.609	■	00-002-0242
67.775	■	00-002-0242
77.532	■	00-002-0242
83.277	■	00-002-0242

the X-ray diffusion method using the Debye–Scherrer equation ($D = 0.9\lambda/\beta_{1/2}\cos\theta$). In this equation, parameters D , λ , β and θ are known as the average crystalline

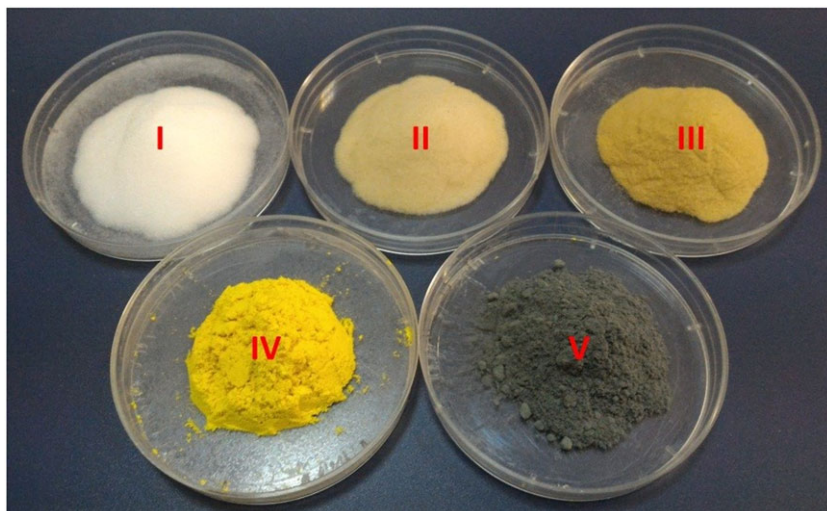


FIGURE 4 Color changes from SiO_2 (I) to STCATSC (V)

size, the X-ray wavelength, the angular line width at half maximum intensity and the Bragg's angle, respectively.^[35] According to copper planes at (111, 200), the average copper crystalline size was measured to be 17.3 nm.

The scanning electron microscopy (SEM) image was used to investigate the size and morphology of the STCATSC. According to Figure 6, catalyst powders are produced at a nano-size, and these particles are aspherical in morphology. Based on the histogram (Figure 7) obtained from the SEM analysis using the microstructural image processing software (MIP software), the particle size distribution was found around 20–25 nm which is in a good agreement and conformity with the data obtained from the XRD analysis. The chemical composition of nanoparticles was also determined using Energy-dispersive X-ray spectroscopy (EDS) (Figure 8). The EDS analysis has allocated the presence of elements C, Si, N, O, S and Cu which are good evidence for synthesis of STCATSC.

The FT-IR spectrum of the STCATSC is shown in Figure 9. The STCATSC is solid and IR spectrum was recorded by the KBr disk technique. The absorption bands displayed in the area of 500 and 600 cm^{-1} are assigned to CuS and CuN bonds, respectively and it is a good witness for formation of complex between thiosemicarbazone and copper.^[36] Furthermore, the reductive shift (i.e.: 41 cm^{-1}) in stretching wavenumber of free thiocarbonyl (i.e.: 756 cm^{-1}) in comparison with that of copper coordinated one in STCATSC (i.e.: 710 cm^{-1}) is an apparent criterion for complex formation between copper and thiocarbonyl residue. A broad band in the 1007–1200 cm^{-1} area is related to the symmetric and anti-symmetric Si-O-Si bond. The C-O bond is shown in a stretching frequency at 1220 cm^{-1} . The peak in the

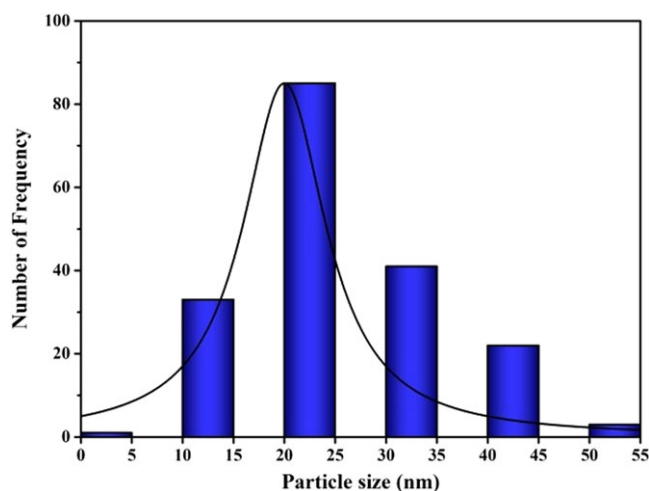


FIGURE 7 Histogram representing the average diameter of STCATSC

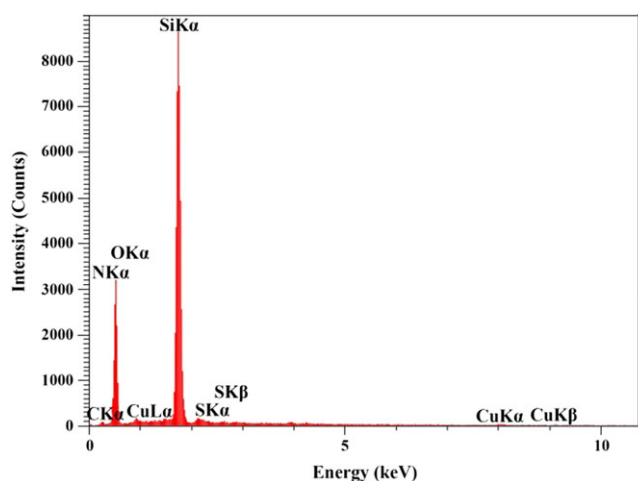


FIGURE 8 EDS Spectrum of STCATSC

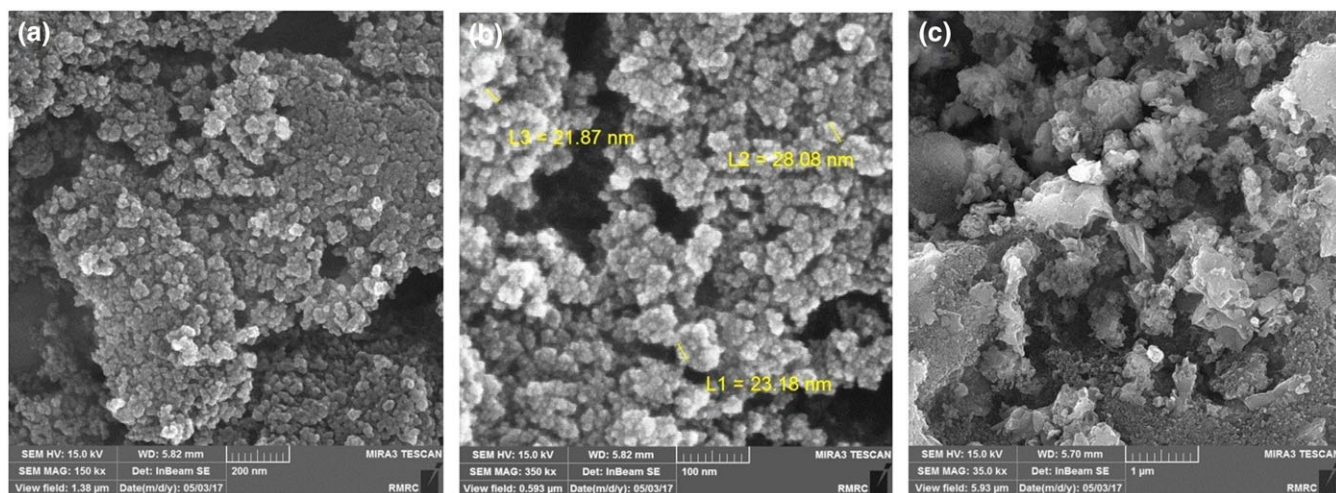


FIGURE 6 Scanning electron microscopy (SEM) image of STCATSC

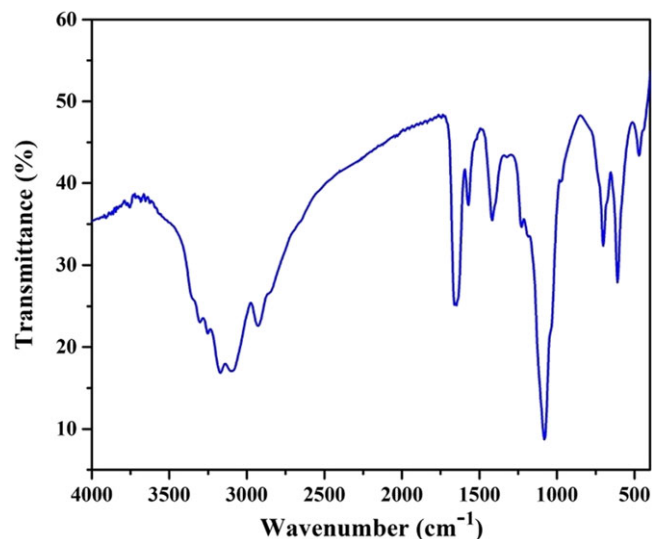


FIGURE 9 FT-IR Spectrum of the STCATSC

region of 1450 cm^{-1} corresponds to methyl moiety (CH_3) bending frequency, and the bands at stretching frequencies of 1600 and 1650 cm^{-1} are attributed to $\text{C}=\text{C}$ and $\text{C}=\text{N}$ bonds, respectively. The absorbance peaks at 2925 and 3100 cm^{-1} are concerned to the aliphatic CH and CH aromatics, accordingly. Two absorbent peaks of NH_2 residue are visible in the area of 3180 and 3350 cm^{-1} . Finally, an absorption band at 3280 cm^{-1} represents NH in STCATSC.

Thermogravimetric (TGA) analysis for STCATSC conducted at weight of sample in heating rate of $10\text{ }^\circ\text{C min}^{-1}$ in N_2 atmosphere within temperature range $26\text{--}600\text{ }^\circ\text{C}$. The thermogram of STCATSC is shown in Figure 10. The thermogram of the catalyst indicates a thermal stability of STCATSC up to $200\text{--}210\text{ }^\circ\text{C}$ with mass loss ($\approx 1\%$) below $100\text{ }^\circ\text{C}$, due to removal of physically adsorbed

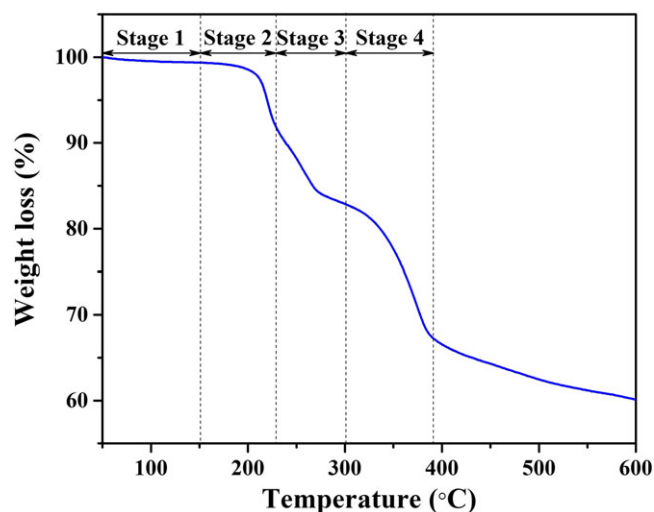
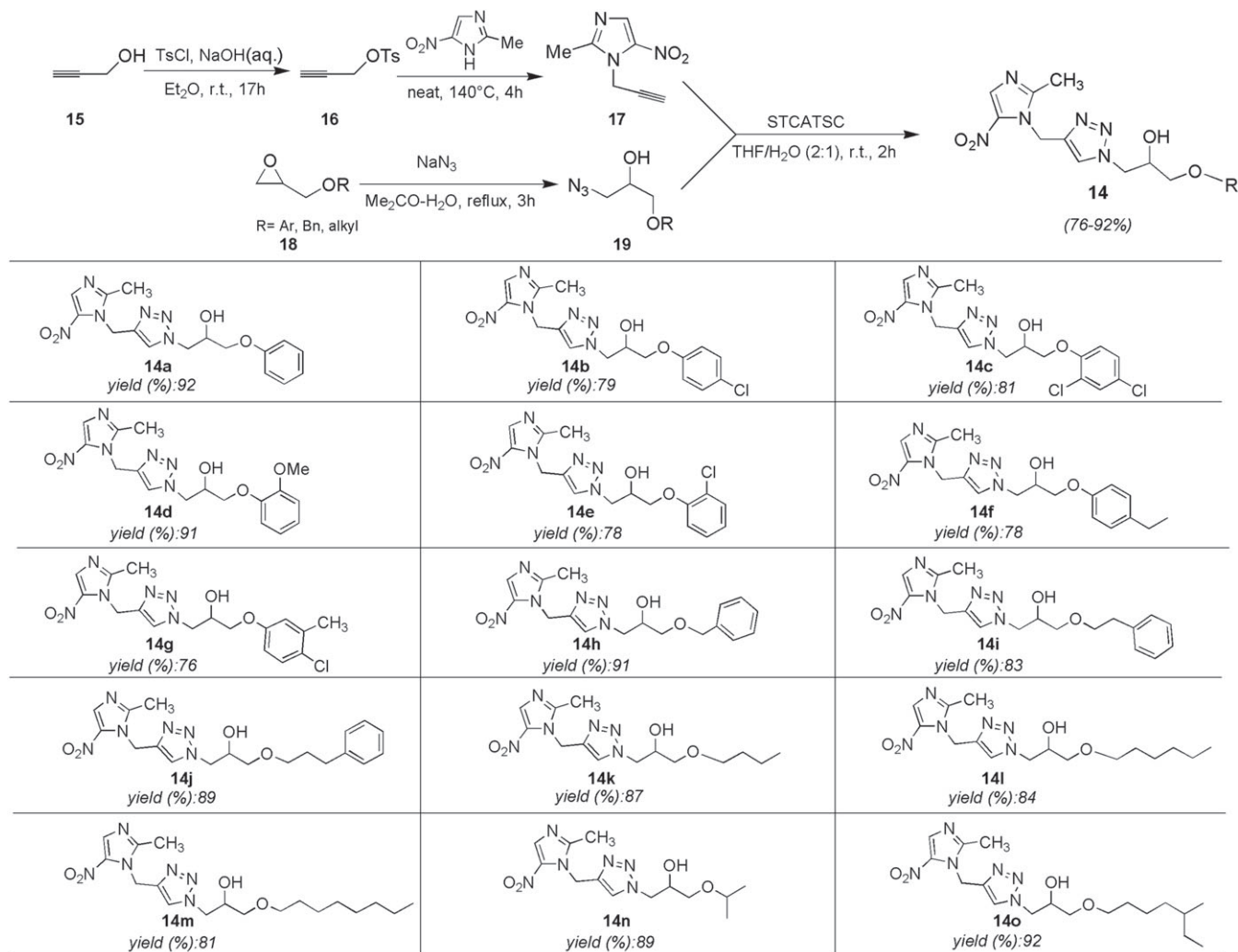


FIGURE 10 Thermogram of STCATSC

water from the sample. As indicated by TGA analysis, the thermal degradation of STCATSC was initiated at a temperature above $215\text{ }^\circ\text{C}$ and the endothermic peaks around $250\text{--}300$ and $350\text{--}400\text{ }^\circ\text{C}$ correspond to decomposition of copper-ligand complex and complete decomposition of grafted organic residue from the surface of silica, respectively. In general, the STCATSC nearly lost 40% of its overall weight at $600\text{ }^\circ\text{C}$ which is a good witness for presence of grafted thiosemicarbazone-copper complex on the surface of silica.

2.3 | Synthesis of 1,2,3-triazolyl-based metronidazole hybrid analogues

The synthetic route to access the title compounds is performed due to general pathway illustrated in Scheme 2. As indicated in Scheme 1, the first step comprises the preparation of propargyl tosylate (**16**) as a propargylating agent from propargyl alcohol (**15**). The use of propargyl tosylate is far superior to propargyl bromide since the propargyl tosylate is a safe and cheap analogue of expensive propargyl bromide which can be easily prepared from tosylation of readily available propargyl alcohol in a mild reaction condition. To this end, we applied a well-established procedure^[37] with a little modification in which the tosyl chloride was used to react with an excess amount of propargyl alcohol in diethyl ether and aqueous NaOH mixture at ambient temperature. This procedure almost provides a quantitative yield of propargyl tosylate ($\approx 100\%$) as yellow oil. Afterward, the synthesized propargyl tosylate (**16**) was utilized to react with 2-methyl-5-nitro-imidazole to access 2-methyl-5-nitro-1-prop-2-ynyl-1*H*-imidazole (**17**) (CAS. NO: 22927-54-4) as a key alkyne in synthesis of target molecule. Since the intrinsic narrow nucleophilic power of 2-methyl-5-nitro-imidazole, the use of basic media can extensively enhance the nucleophilic power and hence the trend in *N*-propargylation of 2-methyl-5-nitro-imidazole, however undesirable 4-nitro isomer of **17** is majorly acquired.^[38] To prevent the formation of 4-nitro isomer adduct, the *N*-propargylation of 2-methyl-5-nitro-imidazole is traditionally achieved in a neutral and/or acidic condition. In this connection, we carried out the *N*-propargylation of 2-methyl-5-nitro-imidazole via **16** under solvent-free condition due to a procedure reported by the literature.^[39] In another synthesis, the different terminal epoxides (**18**) underwent the azidation reaction to afford β -azidoalcohols due to reported standard procedure.^[40] Afterward, through a convergent synthesis using STCATSC, the alkyne (**17**) and β -azidoalcohols (**19**) were used to 'Click' Huisgen cycloaddition reaction in $\text{THF-H}_2\text{O}$ (2:1) media at R.T. to acquire title compounds in



SCHEME 2 Synthesis and structures of 1,2,3-triazolyl-based metronidazole hybrid analogues

good to excellent yields. The structures of synthesized compounds **14a-o** are depicted in Scheme 2. As can be seen in Scheme 2, the main variations were achieved in alkoxy and/or aryloxy moieties which can affect the pharmacokinetic profiles of title products.

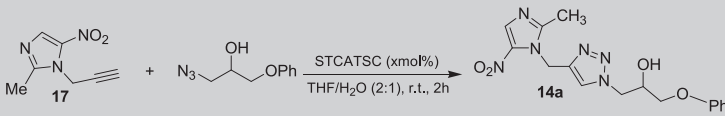
2.4 | The effect of STCATSC amount

Based on the inductively coupled plasma (ICP) analysis, it was indicated that in each gram of catalyst, there are 0.021 g of active Cu catalyst (0.033 mol%). To determine the optimized amount of STCATSC, different amounts of catalyst were examined on cycloaddition reaction of **17** with 1-azido-3-phenoxy-propan-2-ol as a sample reaction to afford **14a** (Table 2). As depicted in Table 2, the best result was obtained when 0.003 mol% or nearly 0.1 g of catalyst was loaded (Table 2, Entry 3). The use

of excess amounts of catalyst has a negligible effect on the progress of the reaction.

2.5 | The reusability of STCATSC

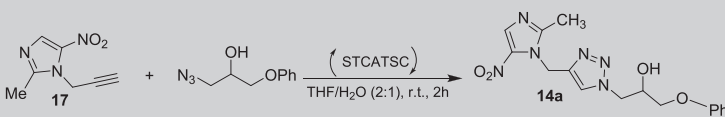
To evaluate the reusability of catalyst, STCATSC was examined in synthesis of compound **14a** as a model reaction after several consecutive runs. In this regard, after each run, the reaction mixture was vacuum-filtered through a sintered-glass funnel, and the remaining solid was washed successively with anhydrous THF and dried in a vacuum oven at 80 °C for 30 min. The catalyst was then reused directly without further purification, and no fresh catalyst was added in subsequent runs. The catalyst was tested in five sequential runs which the results are recorded in Table 3. According to the results (Table 3), the STCATSC can be recycled and reused for many consecutive trials without significant loss of its activity. In

TABLE 2 Influence of catalyst amount in synthesis of **14a** using STCATSC at room temperature^a


Entry	STCATSC (mol %)	Time (h)	Yield (%) ^b
1	0.001	2	75
2	0.002	2	88
3	0.003	2	92
4	0.004	2	92
5	0.005	2	92
6	0.006	2	91
7	0.007	2	91

^aReagents and conditions: **17** (0.01 mol), 1-azido-3-phenoxy-propan-2-ol (0.012 mol), STCATSC (xmol %), THF/H₂O (2:1, 30 ml), room temperature, 2 hr.

^bYield of isolated product.

TABLE 3 The reusability of STCATSC in successive trails for synthesis of **14a**^a


Run	Time (h)	Yield (%) ^b
1	2	92 ^c
2	2	92
3	2	90
4	2	87
5	2	86

^aReagents and conditions: **17** (0.01 mol), 1-azido-3-phenoxy-propan-2-ol (0.012 mol), STCATSC (0.0033 mol%), THF/H₂O (2:1, 30 ml), room temperature, 2 hr.

^bYield of isolated product

^cFresh catalyst

addition, the ICP analysis has indicated the reusability of the STCATSC without considerable desorption of Cu species from silica-thiosemicarbazone matrix. The ICP analysis determined that the amount of leached Cu from STCATSC is extremely negligible (0.006% after five consecutive runs), and it is rationalized due to a strong binding present between the Cu species and thiosemicarbazone on the surface of silica.

2.6 | Antigiardial assessment

Giardia lamblia (*G. lamblia*), also known as *Giardia duodenalis* or *Giardia intestinalis*, is an anaerobic protozoan parasite of the small intestine that causes extensive

morbidity worldwide. Annually, around 280 million human infections in both endemic and epidemic are estimated to occur global.^[41] A disease Giardiasis caused by *G. lamblia* is the most common source of waterborne diarrheal disease, with adults and children in day care centers. Contagious infection is commonly transmitted by fecal-oral transmission and is initiated by ingestion of infectious cysts in contaminated water or through person to person contact. Giardiasis is responsible for the acute symptoms like severe diarrhea, vomiting, nausea, bloating, belching, anorexia, indigestion, abdominal pain, and weight loss. To remedy the giardiasis, MTZ (**2**) as well as its NIMs analogues are most prescribed drugs, however MTZ-resistance giardiasis is observed in some refractory giardia subcategory.^[42] In addition, MTZ can

produce several adverse effects such as nausea, headache, metallic taste, vomiting and dry mouth in some patients. In this connection, the anti-giardial activity of compounds **14a-o** is assessed *in vitro* to indicate their potency in devastating this protozoan parasite. To this end, fecal samples containing cysts of *Giardia intestinalis* from the infected patients were transferred to the Laboratory of Parasitology at Fasa University of Medical Sciences in clean plastic containers. To harvest cysts from stool debris, the cysts were floated using Sheather's sugar flotation procedure. To do it, 1 ml feces was emulsified in 10 to 12 ml normal saline, and filtered then through two layers of moist gauze into a centrifuge tube. The suspension was centrifuged at $900 \times g$; and supernatant was poured off and resuspended in fresh saline. The centrifuge was done again 1 minute at $900 \times g$; if supernatant was still cloudy, the washing was repeated. The 1 to 2 ml fecal suspension was placed in 13 ml conical centrifuge tube and Sheather's sugar flotation was added until tube was three-quarters full and was stirred with applicator stick, vigorously. The tube was filled with sugar solution to 1 or 2 cm from top. The tube was centrifuged at $500 \times g$ for 10 min. To remove the sucrose solution, the harvested cysts were diluted in 1 ml sterile tap water, centrifuged and washed in saline solution 2 times, repeatedly. The washed cysts were stored at 4°C until use for biological assays. Eosin solution (0.001 M) was used for staining live cysts. Number of viable cysts (negative staining by eosin) in $10\ \mu\text{L}$ were determined by hemocytometer method. A solution of different concentrations of metronidazole as a reference drug and **14a-o** (1, 2, 4 and 8 mM) in DMSO (1 mL) were added to a $100\ \mu\text{L}$ suspension of cysts in eppendorf tubes and the tubes maintained at 37°C for 24, 48 and 72 hr. Anti-giardiasis effects of **14a-o** were determined by hemocytometer slide. Each compound in different concentrations was tested against the *Giardia* cysts which the results are depicted in Table 4.

As can be seen in Table 4, the anti-giardiasis investigation of compounds **14a-o** was carried out at different concentrations comprising 1, 2, 4 and 8 mM and obtained data were compared to MTZ as a standard drug in terms of concentration condition. Due to Table 4, at the initial concentration (i.e.: 1 Mm), **14b** displayed similar anti-giardiasis activity compare to MTZ, whereas **14e**, **14 h**, **14i**, **14j**, **14 l**, **14 m** and **14o** demonstrated more activity regarding to MTZ. Nevertheless, at 2 mM concentration, **14i** and **14j** merely exhibited more anti-giardial potency than MTZ. Furthermore, although at 4 mM compound **14e** has shown the same activity as MTZ, however **14 g-j**, **14 l** and **14o** afforded stronger potency than MTZ and finally, at 8 mM **14i**, **14j**, **14 l** and **14o** showed a similar activity profile to MTZ.

TABLE 4 *In vitro* anti-giardial study of **14a-o**

Compound	Mean of Mortality (%)			
	1 ^a	2 ^a	4 ^a	8 ^a
14a	45	65	70	77
14b	69	75	80	82
14c	62	80	84	85
14d	65	78	81	82
14e	80	85	90	92
14f	62	70	73	75
14 g	65	78	91	92
14 h	77	87	92	94
14i	70	90	92	95
14j	80	90	94	95
14 k	42	55	60	70
14 l	78	85	93	95
14 m	77	85	87	93
14n	44	52	65	70
14o	78	84	91	95
MTZ ^b	69	89	90	95

^aConcentrations in mM.

^bMetronidazole as a reference drug

In general, among tested compounds, **14i** and **14j** are the most potent compounds at all tested concentrations, particularly in lower concentrations compare to MTZ.

As shown in Scheme 2, **14a-o** are significantly resemble in their structures and the main variation in functionalities are restricted to aryloxy and/or alkoxy moieties. As stated earlier, although the main pharmacophoric residue of NIM-drugs are NIM cores, however the changes in *N*-alkyl residue of NIMs affects the redox potential and thus alters the antiprotozoal activity. In confirmation of this concept, it was observed that the alteration in aryloxy and/or alkoxy moieties in **14a-o** also affected the anti-giardial potency. Regardless of aryloxy and/or alkoxy moieties' type in **14a-o**, the anti-giardial profiles of all compounds are often considerable. With a few exceptions in obtained data at tested concentrations, compounds **14a-g** involving aryloxy residues bearing both electron-donating and electron-withdrawing groups displayed weaker anti-giardial activity in comparison with MTZ. The progressive trend in anti-giardial activity was observed when the aryloxy residue was changed to benzyloxy, phenethyloxy and phenpropyloxy (**14 h-j**) in which compound **14j** is the most potent anti-giardial agent compare to MTZ. The variation in alkoxy residues from linear aliphatic alkoxy to branched residues provides the

changes in activity in which compound **14 I** and **14o** showed appropriate anti-giardial activity.

3 | CONCLUSION

In summary, the fabrication, characterization and application of silica-tethered cuprous acetophenone thiosemicarbazone (STCATSC) as a novel nano hybrid catalyst for synthesis of new 1,2,3-triazolyl-based metronidazole hybrid analogues has been described. The STCATSC was used in very mild and highly efficient synthesis of new 1,2,3-triazolyl-based metronidazole hybrid analogues. The STCATSC utilized in the facile 'Click' Huisgen cycloaddition reaction of 2-methyl-5-nitro-1-prop-2-ynyl-1H-imidazole (**17**) with diverse β -azidoalcohols (**19**) in THF/H₂O (2:1) media at R.T. to acquire title products in good to excellent yields. STCATSC was proved to be an efficient hybrid catalyst with thermal and chemical stability. This catalyst is a low cost and environmentally benign that can be simply prepared and reused for many reaction runs without a significant decline in its reactivity. 1,2,3-Triazolyl-based metronidazole hybrid analogues (**14a-o**) were *in vitro* tested against Giardia lamblia (G. lamblia). The obtained data was indicated that all compounds displayed varied promising anti-giardial activity compare to MTZ at different concentrations of **14a-o** solutions. Among studied compounds, **14i** and **14j** demonstrated potent anti-giardial activity even stronger than MTZ.

4 | EXPERIMENTAL

4.1 | General

All chemicals were purchased from Merck or Sigma-Aldrich. Solvents were purified by standard procedures, and stored over 3 Å molecular sieves. Reactions were followed by TLC using SILG/UV 254 silica-gel plates. Column chromatography was performed on silica gel 60 (0.063–0.200 mm, 70–230 mesh; ASTM). IR spectra were obtained using a Shimadzu FT-IR-8300 spectrophotometer. GC/MS was performed on a Shimadzu GC/MS-QP 1000-EX apparatus (m/z; rel.%). Elemental analyses were performed on a Perkin-Elmer 240-B micro-analyzer. ¹H- and ¹³C-NMR spectrum was recorded on Brüker Avance-DPX-250/400 spectrometer operating at 300/75 MHz, respectively. Chemical shifts are given in δ relative to tetramethylsilane (TMS) as an internal standard, coupling constants *J* are given in Hz. The scanning electron micrograph was achieved using SEM (VEGA//TESCAN-LMU) instrument. The patterned X-ray diffraction (XRD) was obtained using X'PERT PRO MPD Panalytical. The TGA test was performed using

METTLER TOLEDO instrument. Data involving InChI (Key), ¹HNMR and ¹³CNMR for all products can be found in supporting information section.

4.2 | General procedure for synthesis of STCATSC

In a tubing thermal furnace (internal diameter: 2.0 cm, length: 25 cm), a sample of normal silica gel (5.0 g) was exposed to a flow of 8% O₂ in an argon atmosphere for 1 hr at 400 °C in which afforded the activated SiO₂ (**I**) (Scheme 1). Silica chloride was then prepared by the method described in the literature.^[34] Afterward, to a double-necked round bottom flask (100 ml) equipped with a condenser was added a mixture of 4-hydroxyacetophenone (2.04 g, 15 mmol) and trimethylamine (2.02 g, 20 mmol) in anhydrous toluene (50 ml). The silica chloride (5.3 g) was then added portionwise during 30 minutes at room temperature. The reaction mixture was then refluxed for 48 hr. Subsequently, the suspension was filtered and the solid was washed with anhydrous toluene (3 × 10 ml). The solid was then kept in a vacuum oven at 50 °C for a night to afford silica-4-hydroxyacetophenone adduct **III** as a creamy solid. To prepare silica-thiosemicarbazone adduct (**IV**), it was added a mixture of adduct **III** (2.0 g), thiosemicarbazide (1.09 g, 12 mmol), acetic acid (4 drops), and ethanol (20 ml) in a double-necked round bottom flask (100 ml) equipped with a condenser. The reaction mixture was then heated at reflux for 24 hr. Afterward, the reaction mixture was filtered and the remaining solid was washed with ethanol (3 × 10 ml). The silica-thiosemicarbazone adduct **IV** was obtained as a yellow solid which was kept in a vacuum oven at 50 °C for 6 hr. Then, to a round bottom flask (100 ml), it was charged a mixture containing the adduct **IV** (1.5 g), CuSO₄·5H₂O (2.49 g, 10 mmol) and KI (1.5 g, 9 mmol) in distilled water (30 ml) in which was vigorously stirred at room temperature for 48 hr. Afterward, the suspension was filtered and the solid was washed with distilled water (3 × 10 ml). Finally, the solid was then kept in a vacuum oven at 100 °C for a night to afford adduct **V** as a grey solid.

4.3 | General procedure for synthesis of propargyl tosylate (**16**)^[37]

The propargyl tosylate (**16**) was prepared due to a well-established procedure with a little modification.^[37] In a round bottomed flask (100 ml) equipped with a mechanical stirrer was added propargyl alcohol (0.01 mol), tosyl chloride (0.02 mol) and diethyl ether (25 ml). The resulting reaction mixture was cooled in an ice bath,

and NaOH (2 g, 0.05 mol) pellets were added to the solution in 6 portions at 0 °C under vigorous stirring. Afterward of the reaction completion (TLC control) and the evaporation of the organic solvent, the residue was dissolved in CHCl₃ (150 ml) and washed with H₂O (3 × 150 ml). The organic layer was dried (Na₂SO₄, 10 g) and concentrated to afford the crude product, which was pure enough to use for the subsequent reaction without further purification.

4.4 | General procedure for synthesis of 2-methyl-5-nitro-1-(prop-2-ynyl)-1H-imidazole (17)

Compound **17** was prepared due to the established procedure in the literature.^[39]

4.5 | General procedure for synthesis of β-azido alcohols (19)

β-Azido alcohols were prepared by the method described in the literature.^[30]

4.6 | General procedure for synthesis of 1,2,3-triazolyl-based metronidazole hybrid analogues (14a-o)

In a round-bottomed flask (100 ml) was added a mixture of alkyne **17** (10 mmol), proper β-azido alcohol (14 mmol) and STCATSC (0.1 g) in H₂O/THF (1:2 V/V, 18 mL). The reaction mixture was stirred at room temperature until TLC monitoring indicated no further progress of the reaction (2 hr). Afterward, the catalyst was filtered and the filtrate was then evaporated using vacuum to separate the solvent from the product. The residue was then dissolved in CHCl₃ (150 ml) and washed with H₂O (2 × 150 mL). The organic layer was dried using Na₂SO₄ and evaporated to afford the crude product which was purified by column chromatography on silica gel.

4.7 | Data for new compounds

4.7.1 | 1-(4-((2-methyl-5-nitro-1H-imidazol-1-yl)methyl)-1H-1,2,3-triazol-1-yl)-3-phenoxypropan-2-ol (14a)

Column Chromatography on silica gel eluted with EtOAc afforded pure product as white solid (3.29 g, 92%); m.p. 131–132 °C. IR (KBr): 3300, 3100, 2950, 1550, 1481, 1430, 1350, 1250 cm⁻¹. ¹H NMR (DMSO-*d*₆, 300 MHz) δ_{ppm} = 8.29 (s, 1H, C(4)-H of imidazole) 8.18 (s, 1H,

C(5)-H of triazole), 7.29–7.18 (m, 2H, aryl), 6.94–6.80 (m, 3H, aryl), 5.59–5.52 (m, 1H, CHOH), 5.34 (s, 2H, NCH₂), 4.61 (dd, *J* = 3.6, 13.8 Hz, 1H, OCH_AH_B), 4.46 (dd, *J* = 7.5, 13.8 Hz, 1H, OCH_AH_B) 4.20 (br s, 1H, OH), 3.91–3.84 (m, 2H, NCH₂), 2.39 (s, 3H, CH₃). ¹³C NMR (DMSO-*d*₆, 75 MHz) δ_{ppm} = 163.17 (ArC-O), 159.15 (C(2) of imidazole), 143.67 (C(2) of triazole), 138.78 (C(5) of imidazole), 135.04 (C(4) of imidazole), 132.17 (ArC), 129.88 (C(5) of triazole), 121.25 (ArC), 115.80 (ArC), 78.46 (OCH₂), 70.16 (CHOH), 57.82 (NCH₂CH), 43.18 (NCH₂C=C), 7.85 (CH₃). MS (EI): *m/z* (%) = 358 (23.5) [M⁺]. Anal. Calc. for C₁₆H₁₈N₆O₄: C, 53.63; H, 5.06; N, 23.45; found: C, 53.75; H, 5.19; N, 23.32.

4.7.2 | 1-(4-chlorophenoxy)-3-(4-((2-methyl-5-nitro-1H-imidazol-1-yl)methyl)-1H-1,2,3-triazol-1-yl) propan-2-ol (14b)

Column Chromatography on silica gel eluted with EtOAc afforded pure product as creamy solid (3.10 g, 79%); m.p. 137–138 °C. IR (KBr): 3210, 3150, 2958, 1560, 1476, 1432, 1360, 1260, 825 cm⁻¹. ¹H NMR (CDCl₃, 300 MHz) δ_{ppm} = 7.84 (complex, 2H, C(4)-H of imidazole, C(5)-H of triazole), 7.25–7.21 (m, 2H, aryl), 6.81 (d, *J* = 8.7 Hz, 2H, aryl), 5.57 (s, 2H, NCH₂), 4.68 (dd, *J* = 3.3, 13.8 Hz, 1H, OCH_AH_B), 4.52 (dd, *J* = 7.2, 13.8 Hz, 1H, OCH_AH_B), 4.38 (br s, 1H, OH), 3.97–3.87 (m, 2H, NCH₂), 3.59–3.58 (m, 1H, CHOH), 2.71 (s, 3H, CH₃). ¹³C NMR (CDCl₃, 75 MHz) δ_{ppm} = 163.16 (ArC-O), 157.13 (C(2) of imidazole), 144.25 (C(4) of triazole), 139.08 (C(5) of imidazole), 135.65 (ArC), 132.78 (C(4) of imidazole), 130.22 (ArC-Cl), 126.19 (C(5) of triazole), 116.17 (ArC), 78.37 (OCH₂), 70.34 (CHOH), 58.02 (NCH₂CH), 43.69 (NCH₂C=C), 7.60 (CH₃). MS (EI): *m/z* (%) = 392 (27.1) [M⁺]. Anal. Calc. for C₁₆H₁₇ClN₆O₄: C, 48.92; H, 4.36; N, 21.40; found: C, 49.06; H, 4.25; N, 21.54.

4.7.3 | 1-(2,4-dichlorophenoxy)-3-(4-((2-methyl-5-nitro-1H-imidazol-1-yl)methyl)-1H-1,2,3-triazol-1-yl)propan-2-ol (14c)

Column Chromatography on silica gel eluted with EtOAc afforded pure product as white solid (3.46 g, 81%); m.p. 163–164 °C. IR (KBr): 3225, 3025, 2950, 1550, 1480, 1435, 1350, 1290, 1060, 740 cm⁻¹. ¹H NMR (CDCl₃, 300 MHz) δ_{ppm} = 7.73 (complex, 2H, C(4)-H of imidazole, C(5)-H of triazole), 7.37–7.32 (m, 3H, aryl), 5.20 (s, 2H, NCH₂), 4.76 (dd, *J* = 2.7, 13.2 Hz, 1H, OCH_AH_B), 4.62 (dd, *J* = 6.6, 14.4 Hz, 1H, OCH_AH_B), 4.46 (br s, 1H, OH), 4.05–3.91 (m, 2H, NCH₂), 3.46–3.45 (m, 1H, CHOH), 2.50 (s, 3H, CH₃). ¹³C NMR (CDCl₃, 75 MHz) δ_{ppm} = 163.34 (C(2) of imidazole), 158.09 (ArC-O),

143.98 (C(4) of triazole), 139.05 (C(5) of imidazole), 134.95 (ArC), 132.27 (C(4) of imidazole), 130.53 (ArC), 128.23 (ArC-Cl), 127.59 (ArC-Cl), 121.18 (C(5) of triazole), 118.25 (ArC), 77.86 (OCH₂), 70.20 (CHOH), 58.80 (NCH₂CH), 41.22 (NCH₂C=C), 6.99 (CH₃). MS (EI): *m/z* (%) = 426 (38.4) [M⁺]. Anal. Calc. for C₁₆H₁₆Cl₂N₆O₄: C, 44.98; H, 3.77; N, 19.67; found: C, 45.12; H, 3.90; N, 19.83.

4.7.4 | 1-(2-methoxyphenoxy)-3-(4-((2-methyl-5-nitro-1*H*-imidazol-1-yl)methyl)-1*H*-1,2,3-triazol-1-yl) propan-2-ol (14d)

Column Chromatography on silica gel eluted with EtOAc afforded pure product as white solid (3.53 g, 91%); m.p. 152–153 °C. IR (KBr): 3200, 3050, 2954, 1550, 1465, 1425, 1351, 1248, 1045 cm⁻¹. ¹H NMR (CDCl₃, 300 MHz) δ_{ppm} = 7.74 (s, 1H, C(4)-H of imidazole), 7.72 (s, 1H, C(5)-H of triazole), 7.25–7.17 (m, 2H, aryl), 6.91–6.89 (m, 2H, aryl), 5.19 (s, 2H, NCH₂), 4.72 (dd, *J* = 3.3, 13.8 Hz, 1H, OCH_AH_B), 4.57 (dd, *J* = 6.9, 14.1 Hz, 1H, OCH_AH_B), 4.36 (br s, 1H, OH), 4.07–4.02 (m, 2H, NCH₂), 3.92–3.87 (m, 1H, CHOH), 3.84 (s, 3H, OCH₃), 2.48 (s, 3H, CH₃). ¹³C NMR (CDCl₃, 75 MHz) δ_{ppm} = 162.97 (C(2) of imidazole), 148.22 (ArC-OCH₃), 145.20 (ArC-OCH₂), 144.30 (C(4) of triazole), 139.47 (C(5) of imidazole), 135.55 (C(4) of imidazole), 132.22 (C(5) of triazole), 123.19 (ArC), 122.89 (ArC), 115.97 (ArC), 113.22 (ArC), 78.58 (OCH₂), 70.43 (CHOH), 58.09 (NCH₂CH), 57.48 (OCH₃), 43.63 (NCH₂C=C), 8.05 (CH₃). MS (EI): *m/z* (%) = 388 (21.6) [M⁺]. Anal. Calc. for C₁₇H₂₀N₆O₅: C, 52.57; H, 5.19; N, 21.64; found: C, 52.41; H, 5.02; N, 21.50.

4.7.5 | 1-(2-chlorophenoxy)-3-(4-((2-methyl-5-nitro-1*H*-imidazol-1-yl)methyl)-1*H*-1,2,3-triazol-1-yl) propan-2-ol (14e)

Column Chromatography on silica gel eluted with EtOAc afforded pure product as yellow solid (3.06 g, 78%); m.p. 106–107 °C. IR (KBr): 3225, 3125, 2900, 1551, 1489, 1435, 1354, 1243, 1060, 750 cm⁻¹. ¹H NMR (CDCl₃, 300 MHz) δ_{ppm} = 7.76 (s, 1H, C(4)-H of imidazole), 7.71 (s, 1H, C(5)-H of triazole), 7.37 (d, *J* = 7.8 Hz, 1H, aryl), 7.25–7.17 (m, 2H, aryl), 6.97–6.87 (m, 1H, aryl), 5.18 (s, 2H, NCH₂), 4.78 (dd, *J* = 3.3, 14.1 Hz, 1H, OCH_AH_B), 4.65 (dd, *J* = 6.9, 14.1 Hz, 1H, OCH_AH_B), 4.48 (br s, 1H, OH), 4.06–3.95 (complex, 3H, NCH₂CH), 2.46 (s, 3H, CH₃). ¹³C NMR (CDCl₃, 75 MHz) δ_{ppm} = 163.82 (C(2) of imidazole), 159.87 (ArC-O), 144.23 (C(4) of triazole), 139.11 (C(5) of imidazole), 135.13 (ArC), 132.87 (C(4) of imidazole), 130.62 (ArC),

128.05 (C(5) of triazole), 121.81 (ArC-Cl), 120.10 (ArC), 116.14 (ArC), 78.05 (OCH₂), 70.67 (CHOH), 58.46 (NCH₂CH), 43.11 (NCH₂C=C), 5.61 (CH₃). MS (EI): *m/z* (%) = 392 (31.9) [M⁺]. Anal. Calc. for C₁₆H₁₇ClN₆O₄: C, 48.92; H, 4.36; N, 21.40; found: C, 49.03; H, 4.47; N, 21.51.

4.7.6 | 1-(4-ethylphenoxy)-3-(4-((2-methyl-5-nitro-1*H*-imidazol-1-yl)methyl)-1*H*-1,2,3-triazol-1-yl)propan-2-ol (14f)

Column Chromatography on silica gel eluted with EtOAc afforded pure product as white solid (3.01 g, 78%); m.p. 115–116 °C. IR (KBr): 3290, 3100, 2957, 1552, 1490, 1430, 1351, 1245, 1050 cm⁻¹. ¹H NMR (CDCl₃, 300 MHz) δ_{ppm} = 7.77 (s, 1H, C(4)-H of imidazole), 7.73 (s, 1H, C(5)-H of triazole), 7.11 (d, *J* = 8.7 Hz, 2H, aryl), 6.80 (d, *J* = 8.4 Hz, 2H, aryl), 5.17 (s, 2H, NCH₂), 4.74 (dd, *J* = 3.0, 14.1 Hz, 1H, OCH_AH_B), 4.55 (dd, *J* = 7.5, 14.1 Hz, 1H, OCH_AH_B), 4.40 (br s, 1H, OH), 4.00–3.88 (m, 2H, NCH₂), 3.71–3.70 (m, 1H, CHOH), 2.61 (q, *J* = 7.5 Hz, 2H, CH₂CH₃), 2.45 (s, 3H, CH₃), 1.21 (t, *J* = 7.5 Hz, 3H, CH₂CH₃). ¹³C NMR (CDCl₃, 75 MHz) δ_{ppm} = 163.28 (ArC-O), 159.99 (C(2) of imidazole), 144.80 (C(4) of triazole), 139.11 (C(5) of imidazole), 135.69 (ArC-Et), 132.58 (C(4) of imidazole), 132.02 (ArC), 128.86 (C(5) of triazole), 114.66 (ArC), 78.61 (OCH₂), 70.09 (CHOH), 57.60 (NCH₂CH), 43.39 (NCH₂C=C), 29.18 (CH₂CH₃), 17.54 (CH₂CH₃), 6.76 (CH₃). MS (EI): *m/z* (%) = 386 (18.2) [M⁺]. Anal. Calc. for C₁₈H₂₂N₆O₄: C, 55.95; H, 5.74; N, 21.75; found: C, 56.10; H, 5.89; N, 21.86.

4.7.7 | 1-(4-chloro-3-methylphenoxy)-3-(4-((2-methyl-5-nitro-1*H*-imidazol-1-yl)methyl)-1*H*-1,2,3-triazol-1-yl)propan-2-ol (14 g)

Column Chromatography on silica gel eluted with EtOAc afforded pure product as white solid (3.09 g, 76%); m.p. 162–163 °C. IR (KBr): 3350, 3075, 2950, 1556, 1485, 1425, 1351, 1240, 1045, 758 cm⁻¹. ¹H NMR (CDCl₃, 300 MHz) δ_{ppm} = 7.73 (s, 1H, C(4)-H of imidazole), 7.71 (s, 1H, C(5)-H of triazole), 7.25–7.18 (m, 2H, aryl), 6.76 (s, 1H, aryl), 5.21 (s, H, NCH₂), 4.73 (dd, *J* = 3.0, 14.4 Hz, 1H, OCH_AH_B), 4.57 (dd, *J* = 6.9, 14.1 Hz, 1H, OCH_AH_B), 4.18 (br s, H, OH), 4.02–3.84 (complex, 3H, NCH₂CH), 2.50 (s, 3H, CH₃), 1.55 (s, 3H, PhCH₃). ¹³C NMR (CDCl₃, 75 MHz) δ_{ppm} = 163.62 (ArC-O), 157.21 (C(2) of imidazole), 144.30 (C(4) of triazole), 139.91 (C(5) of imidazole), 139.05 (ArC-Me), 136.10 (ArC), 132.91 (C(4) of imidazole), 130.24 (ArC-

Cl), 127.33 (C(5) of triazole), 117.37 (ArC), 113.58 (ArC), 79.03 (OCH₂), 71.09 (CHOH), 58.21 (NCH₂CH), 43.28 (NCH₂C=C), 13.11 (ArC-CH₃), 7.25 (CH₃). MS (EI): *m/z* (%) = 406 (25.3) [M⁺]. Anal. Calc. for C₁₇H₁₉ClN₆O₄: C, 50.19; H, 4.71; N, 20.66; found: C, 50.27; H, 4.60; N, 20.54.

4.7.8 | 1-(benzyloxy)-3-(4-((2-methyl-5-nitro-1*H*-imidazol-1-yl)methyl)-1*H*-1,2,3-triazol-1-yl)propan-2-ol (14 h)

Column Chromatography on silica gel eluted with EtOAc afforded pure product as yellow oil (3.38 g, 91%). IR (film): 3350, 3100, 2960, 1550, 1472, 1430, 1350, 1125 cm⁻¹. ¹H NMR (CDCl₃, 300 MHz) δ_{ppm} = 7.70 (complex, 2H, C(4)-H of imidazole, C(5)-H of triazole), 7.31–7.25 (m, 5H, aryl), 5.14 (s, 2H, NCH₂), 4.58–4.35 (complex, 4H, OCH₂, PhCH₂), 4.18 (br s, 1H, OH), 3.55–3.33 (complex, 3H, NCH₂CH), 2.44 (s, 3H, CH₃). ¹³C NMR (CDCl₃, 75 MHz) δ_{ppm} = 163.54 (C(2) of imidazole), 144.80 (C(4) of triazole), 139.69 (C(5) of imidazole), 138.26 (ArC-CH₂), 135.41 (ArC), 132.87 (ArC), 130.90 (C(4) of imidazole), 129.47 (ArC), 128.61 (C(5) of triazole), 76.35 (ArC-CH₂O), 75.20 (OCH₂), 70.67 (CHOH), 58.17 (NCH₂CH), 43.11 (NCH₂C=C), 6.76 (CH₃). MS (EI): *m/z* (%) = 372 (17.5) [M⁺]. Anal. Calc. for C₁₇H₂₀N₆O₄: C, 54.83; H, 5.41; N, 22.57; found: C, 54.97; H, 5.30; N, 22.61.

4.7.9 | 1-(4-((2-methyl-5-nitro-1*H*-imidazol-1-yl)methyl)-1*H*-1,2,3-triazol-1-yl)-3-phenethoxypropan-2-ol (14i)

Column Chromatography on silica gel eluted with EtOAc afforded pure product as yellow solid (3.20 g, 83%); m.p. 64–65 °C. IR (KBr): 3350, 3090, 2956, 1550, 1486, 1420, 1352, 1258 cm⁻¹. ¹H NMR (CDCl₃, 300 MHz) δ_{ppm} = 7.71 (s, 1H, C(4)-H of imidazole), 7.51 (s, 1H, C(5)-H of triazole), 7.30–7.18 (m, 5H, aryl), 5.12 (s, 2H, NCH₂), 4.51 (dd, *J* = 3.6, 14.1 Hz, 1H, NCH_AH_B), 4.34 (dd, *J* = 7.2, 14.1 Hz, 1H, NCH_AH_B), 4.11 (br s, 1H, OH), 3.69–3.63 (m, 2H, OCH₂CH), 3.44–3.32 (complex, 3H, PhCH₂CH₂, CHOH), 2.87 (t, *J* = 6.6 Hz, 2H, PhCH₂), 2.44 (s, 3H, CH₃). ¹³C NMR (CDCl₃, 75 MHz) δ_{ppm} = 163.17 (C(2) of imidazole), 143.94 (C(4) of triazole), 141.33 (C(5) of imidazole), 139.05 (ArC-CH₂), 134.18 (ArC), 132.45 (C(4) of imidazole), 129.29 (ArC), 128.17 (ArC), 126.12 (C(5) of triazole), 75.91 (CH₂CH₂O), 73.05 (OCH₂), 70.16 (CHOH), 58.11 (NCH₂CH), 42.88 (NCH₂C=C), 37.17 (ArC-CH₂), 7.29 (CH₃). MS (EI): *m/z* (%) = 386 (18.7) [M⁺]. Anal.

Calc. for C₁₈H₂₂N₆O₄: C, 55.95; H, 5.74; N, 21.75; found: C, 56.11; H, 5.85; N, 21.83.

4.7.10 | 1-(4-((2-methyl-5-nitro-1*H*-imidazol-1-yl)methyl)-1*H*-1,2,3-triazol-1-yl)-3-(3-phenylpropoxy)propan-2-ol (14j)

Column Chromatography on silica gel eluted with EtOAc afforded pure product as yellow oil (3.56 g, 89%). IR (film): 3350, 3095, 2968, 1553, 1493, 1425, 1351, 1125 cm⁻¹. ¹H NMR (CDCl₃, 300 MHz) δ_{ppm} = 7.81 (s, 1H, C(4)-H of imidazole), 7.74 (s, 1H, C(5)-H of triazole), 7.25–7.08 (m, 5H, aryl), 5.12 (s, 2H, NCH₂), 4.55 (dd, *J* = 2.7, 14.1 Hz, 1H, NCH_AH_B), 4.36 (dd, *J* = 7.5, 14.1 Hz, 1H, NCH_AH_B), 4.11 (br s, 1H, OH), 3.42–3.34 (complex, 3H, OCH₂CH), 2.61 (t, *J* = 7.5 Hz, 2H, OCH₂CH₂), 2.37 (s, 3H, CH₃), 1.84 (t, *J* = 8.1 Hz, 2H, PhCH₂), 1.21–1.16 (m, 2H, OCH₂CH₂). ¹³C NMR (CDCl₃, 75 MHz) δ_{ppm} = 163.11 (C(2) of imidazole), 144.70 (C(4) of triazole), 140.49 (C(5) of imidazole), 139.26 (ArC-CH₂), 135.64 (ArC), 133.52 (C(4) of imidazole), 130.50 (ArC), 129.31 (ArC), 126.29 (C(5) of triazole), 76.49 (OCH₂), 72.26 (CH₂CH₂O), 70.77 (CHOH), 58.35 (NCH₂CH), 43.58 (NCH₂C=C), 34.25 (ArC-CH₂), 33.04 (CH₂CH₂O), 5.88 (CH₃). MS (EI): *m/z* (%) = 400 (20.3) [M⁺]. Anal. Calc. for C₁₉H₂₄N₆O₄: C, 56.99; H, 6.04; N, 20.99; found: C, 56.83; H, 6.15; N, 21.10.

4.7.11 | 1-butoxy-3-(4-((2-methyl-5-nitro-1*H*-imidazol-1-yl)methyl)-1*H*-1,2,3-triazol-1-yl)propan-2-ol (14 k)

Column Chromatography on silica gel eluted with EtOAc afforded pure product as brown solid (2.94 g, 87%); m.p. 65–66 °C. IR (KBr): 3275, 3065, 2961, 1550, 1476, 1429, 1351, 1238 cm⁻¹. ¹H NMR (CDCl₃, 300 MHz) δ_{ppm} = 7.78 (s, 1H, C(4)-H of imidazole), 7.74 (s, 1H, C(5)-H of triazole), 5.18 (s, 2H, NCH₂), 4.59 (dd, *J* = 3.0, 14.1 Hz, 1H, NCH_AH_B), 4.41 (dd, *J* = 7.5, 14.1 Hz, 1H, NCH_AH_B), 4.15 (br s, 1H, OH), 3.49–3.33 (m, 5H, CH₂OCH₂CH), 2.46 (s, 3H, CH₃), 1.56–1.47 (m, 2H, OCH₂CH₂), 1.38–1.29 (m, 2H, CH₂CH₃), 0.91 (t, *J* = 7.5 Hz, 3H, CH₂CH₃). ¹³C NMR (CDCl₃, 75 MHz) δ_{ppm} = 162.29 (C(2) of imidazole), 144.23 (C(4) of triazole), 139.05 (C(5) of imidazole), 135.04 (C(4) of imidazole), 132.73 (C(5) of triazole), 76.19 (OCH₂), 71.31 (CH₂CH₂O), 70.74 (CHOH), 58.11 (NCH₂CH), 43.48 (NCH₂C=C), 34.25 (CH₂CH₂O), 21.06 (CH₂CH₃), 15.62 (CH₂CH₃), 7.57 (CH₃). MS (EI): *m/z* (%) = 338 (15.2) [M⁺]. Anal. Calc. for C₁₄H₂₂N₆O₄: C, 49.70; H, 6.55; N, 24.84; found: C, 49.81; H, 6.70; N, 24.98.

4.7.12 | 1-(hexyloxy)-3-(4-((2-methyl-5-nitro-1*H*-imidazol-1-yl)methyl)-1*H*-1,2,3-triazol-1-yl)propan-2-ol (14 l)

Column Chromatography on silica gel eluted with EtOAc afforded pure product as yellow solid (3.07 g, 84%); m.p. 79–80 °C. IR (KBr): 3275, 3080, 2979, 1552, 1480, 1430, 1350, 1175 cm^{-1} . ^1H NMR (CDCl_3 , 300 MHz) δ_{ppm} = 7.79 (s, 1H, C(4)-H of imidazole), 7.74 (s, 1H, C(5)-H of triazole), 5.18 (s, 2H, NCH_2), 4.59 (dd, J = 3.0, 14.1 Hz, 1H, NCH_AH_B), 4.40 (dd, J = 7.5, 13.8 Hz, 1H, NCH_AH_B), 4.15 (br s, 1H, OH), 3.48–3.33 (complex, 5H, $\text{CH}_2\text{OCH}_2\text{CH}$), 2.45 (s, 3H, CH_3), 1.54 (t, J = 6.6 Hz, 2H, OCH_2CH_2), 1.28–1.25 (complex, 6H, $(\text{CH}_2)_3\text{CH}_3$), 0.87 (t, J = 6.0 Hz, 3H, CH_2CH_3). ^{13}C NMR (CDCl_3 , 75 MHz) δ_{ppm} = 163.47 (C(2) of imidazole), 144.23 (C(4) of triazole), 139.34 (C(5) of imidazole), 135.32 (C(4) of imidazole), 132.73 (C(5) of triazole), 76.19 (OCH_2), 71.31 ($\text{CH}_2\text{CH}_2\text{O}$), 70.16 (CHOH), 58.11 (NCH_2CH), 43.18 ($\text{NCH}_2\text{C}=\text{C}$), 33.71 ($\text{CH}_2\text{CH}_2\text{CH}_3$), 31.68 ($\text{CH}_2\text{CH}_2\text{O}$), 27.39 ($\text{CH}_2(\text{CH}_2)_2\text{O}$), 24.23 (CH_2CH_3), 15.04 (CH_2CH_3), 6.14 (CH_3). MS (EI): m/z (%) = 366 (17.8) [M^+]. Anal. Calc. for $\text{C}_{16}\text{H}_{26}\text{N}_6\text{O}_4$: C, 52.45; H, 7.15; N, 22.94; found: C, 52.58; H, 7.26; N, 23.09.

4.7.13 | 1-(4-((2-methyl-5-nitro-1*H*-imidazol-1-yl)methyl)-1*H*-1,2,3-triazol-1-yl)-3-(octyloxy)propan-2-ol (14 m)

Column Chromatography on silica gel eluted with EtOAc afforded pure product as yellow solid (3.19 g, 81%); m.p. 64–65 °C. IR (KBr): 3275, 3067, 2980, 1550, 1495, 1440, 1350, 1128 cm^{-1} . ^1H NMR (CDCl_3 , 300 MHz) δ_{ppm} = 7.77 (s, 1H, C(4)-H of imidazole), 7.74 (s, 1H, C(5)-H of triazole), 5.19 (s, 2H, NCH_2), 4.60 (dd, J = 3.0, 14.1 Hz, 1H, NCH_AH_B), 4.41 (dd, J = 7.5, 14.1 Hz, 1H, NCH_AH_B), 4.15 (br s, 1H, OH), 3.50–3.31 (complex, 5H, $\text{CH}_2\text{OCH}_2\text{CH}$), 2.46 (s, 3H, CH_3), 1.54 (t, J = 6.9 Hz, 2H, OCH_2CH_2), 1.25 (br s, complex, 10H, $(\text{CH}_2)_5\text{CH}_3$), 0.87 (t, J = 6.3 Hz, 3H, CH_2CH_3). ^{13}C NMR (CDCl_3 , 75 MHz) δ_{ppm} = 163.62 (C(2) of imidazole), 144.62 (C(4) of triazole), 139.64 (C(5) of imidazole), 135.23 (C(4) of imidazole), 132.27 (C(5) of triazole), 75.50 (OCH_2), 71.68 ($\text{CH}_2\text{CH}_2\text{O}$), 70.80 (CHOH), 58.21 (NCH_2CH), 41.82 ($\text{NCH}_2\text{C}=\text{C}$), 34.22 ($\text{CH}_2\text{CH}_2\text{CH}_3$), 33.63 ($\text{CH}_2\text{CH}_2\text{O}$), 31.85 ($\text{CH}_2(\text{CH}_2)_3\text{CH}_3$), 31.29 ($\text{CH}_2(\text{CH}_2)_2\text{CH}_3$), 27.47 ($\text{CH}_2(\text{CH}_2)_2\text{O}$), 24.25 (CH_2CH_3), 14.88 (CH_2CH_3), 6.07 (CH_3). MS (EI): m/z (%) = 394 (24.7) [M^+]. Anal. Calc. for $\text{C}_{18}\text{H}_{30}\text{N}_6\text{O}_4$: C, 54.81; H, 7.67; N, 21.30; found: C, 54.95; H, 7.80; N, 21.47.

4.7.14 | 1-isopropoxy-3-(4-((2-methyl-5-nitro-1*H*-imidazol-1-yl)methyl)-1*H*-1,2,3-triazol-1-yl)propan-2-ol (14n)

Column Chromatography on silica gel eluted with EtOAc afforded pure product as white solid (2.88 g, 89%); m.p. 108–109 °C. IR (KBr): 3280, 3085, 2964, 1552, 1476, 1437, 1353, 1167 cm^{-1} . ^1H NMR (CDCl_3 , 300 MHz) δ_{ppm} = 7.79 (s, 1H, C(4)-H of imidazole), 7.74 (s, 1H, C(5)-H of triazole), 5.18 (s, 2H, NCH_2), 4.58 (dd, J = 3.0, 14.1 Hz, 1H, NCH_AH_B), 4.40 (dd, J = 7.2, 13.8 Hz, 1H, NCH_AH_B), 4.10 (br s, 1H, OH), 3.60–3.31 (complex, 4H, CHOCH_2CH), 2.45 (s, 3H, CH_3), 1.11 (d, J = 3.3 Hz, 6H, $\text{CH}(\text{CH}_3)_2$). ^{13}C NMR (CDCl_3 , 75 MHz) δ_{ppm} = 163.13 (C(2) of imidazole), 144.41 (C(4) of triazole), 137.32 (C(5) of imidazole), 134.49 (C(4) of imidazole), 132.50 (C(5) of triazole), 72.04 ($(\text{CH}_3)_2\text{CHO}$), 70.92 (OCH_2), 69.24 (CHOH), 57.91 (NCH_2CH), 43.12 ($\text{NCH}_2\text{C}=\text{C}$), 24.68 ($(\text{CH}_3)_2\text{CH}$), 7.39 (CH_3). MS (EI): m/z (%) = 324 (15.9) [M^+]. Anal. Calc. for $\text{C}_{13}\text{H}_{20}\text{N}_6\text{O}_4$: C, 48.14; H, 6.22; N, 25.91; found: C, 48.02; H, 6.09; N, 25.76.

4.7.15 | 1-(4-((2-methyl-5-nitro-1*H*-imidazol-1-yl)methyl)-1*H*-1,2,3-triazol-1-yl)-3-(5-methylheptyloxy)propan-2-ol (14o)

Column Chromatography on silica gel eluted with EtOAc afforded pure product as yellow oil (3.62 g, 92%). IR (film): 3350, 3100, 2942, 1550, 1489, 1436, 1350, 1237 cm^{-1} . ^1H NMR (CDCl_3 , 300 MHz) δ_{ppm} = 7.80 (s, 1H, C(4)-H of imidazole), 7.75 (s, 1H, C(5)-H of triazole), 5.17 (s, 2H, NCH_2), 4.59 (dd, J = 3.0, 14.1 Hz, 1H, NCH_AH_B), 4.39 (dd, J = 7.8, 14.1 Hz, 1H, NCH_AH_B), 4.15 (br s, 1H, OH), 3.47–3.26 (complex, 5H, $\text{CH}_2\text{OCH}_2\text{CH}$), 2.43 (s, 3H, CH_3), 1.46–1.44 (m, 2H, OCH_2CH_2), 1.32–1.15 (complex, 7H, $\text{CH}_2\text{CH}_2\text{CHCH}_2\text{CH}_3$), 0.84–0.78 (complex, 6H, CHCH_3 , CH_2CH_3). ^{13}C NMR (CDCl_3 , 75 MHz) δ_{ppm} = 163.16 (C(2) of imidazole), 144.25 (C(4) of triazole), 139.08 (C(5) of imidazole), 135.65 (C(4) of imidazole), 133.11 (C(5) of triazole), 76.09 (OCH_2), 71.22 ($\text{CH}_2\text{CH}_2\text{O}$), 70.61 (CHOH), 57.75 (NCH_2CH), 43.14 ($\text{NCH}_2\text{C}=\text{C}$), 38.26 ($\text{CH}_2(\text{CH}_2)_3\text{O}$), 35.11 (CHCH_3), 32.54 (CH_2CH_3), 31.10 ($\text{CH}_2\text{CH}_2\text{O}$), 25.38 ($\text{CH}_2(\text{CH}_2)_2\text{O}$), 20.22 (CHCH_3), 12.49 (CH_2CH_3), 5.61 (CH_3). MS (EI): m/z (%) = 394 (21.7) [M^+]. Anal. Calc. for $\text{C}_{18}\text{H}_{30}\text{N}_6\text{O}_4$: C, 54.81; H, 7.67; N, 21.30; found: C, 54.97; H, 7.78; N, 21.19.

ACKNOWLEDGEMENTS

The authors wish to thank Shiraz University of Technology research council for partial support of this work.

CONFLICT OF INTEREST

The authors declare that they have no conflict of interest.

ORCID

Mohammad Navid Soltani Rad  <https://orcid.org/0000-0002-6000-9053>

REFERENCES

- [1] C. W. Ang, A. M. Jarrad, M. A. Cooper, M. A. T. Blaskovich, *J. Med. Chem.* **2017**, *60*, 7636.
- [2] S. Nakamura, *Pharm. Bull.* **1955**, *3*, 379.
- [3] A. Kleeman, J. Engel, B. Kutscher, D. Reichert, *Pharmaceutical substances*, 3rd ed., Thieme, Stuttgart **1999**.
- [4] A. Mital, *Sci. Pharm.* **2009**, *77*, 497.
- [5] J. Jacobson, S. Bush, *Trends Parasitol.* **2018**, *34*, 175.
- [6] Z. A. Bhutta, J. Sommerfeld, Z. S. Lassi, R. A. Salam, J. K. Das, *Infect. Dis. Poverty* **2014**, *3*, 21.
- [7] C. E. Voogd, *Mutat. Res. Rev. Genet. Toxicol.* **1981**, *86*, 243.
- [8] J. Samuelson, *Antimicrob. Agents Chemother.* **1999**, *43*, 1533.
- [9] R. Sharma, *Curr. Radiopharm.* **2011**, *4*, 379.
- [10] S. Kizaka-Kondoh, H. Konse-Nagasawa, *Cancer Sci.* **2009**, *100*, 1366.
- [11] S. Patterson, S. Wyllie, *Trends Parasitol.* **2014**, *30*, 289.
- [12] D. I. Edwards, *J. Antimicrob. Chemother.* **1993**, *31*, 9.
- [13] A. M. Thompson, M. Bonnet, H. H. Lee, S. G. Franzblau, B. Wan, G. S. Wong, C. B. Cooper, W. A. Denny, *ACS Med. Chem. Lett.* **2017**, *8*, 1275.
- [14] P. Upcroft, J. A. Upcroft, *Clin. Microbiol. Rev.* **2001**, *14*, 150.
- [15] J. A. Upcroft, L. A. Dunn, J. M. Wright, K. Benakli, P. Upcroft, P. Vanelle, *Antimicrob. Agents Chemother.* **2006**, *50*, 344.
- [16] (a) J. H. Boyer, *Nitroazoles*, VCH Publishers, Inc., Deerfield Beach, FL **1986**, p. 165. (b) L. Larina, V. Lopyrev, *Nitroazoles: Synthesis, Structure and Applications (Topics in Applied Chemistry)*, Springer, New York, 2009 edition (**2012**).
- [17] J. E. Moses, A. D. Moorhouse, *Chem. Soc. Rev.* **2007**, *36*, 1249.
- [18] B. Negi, N. Kumar, R. K. Rohilla, N. Roy, D. S. Rawat, *Bioorg. Med. Chem. Lett.* **2009**, *19*, 1396.
- [19] B. Negi, K. K. Raj, S. M. Siddiqui, D. Ramachandran, A. Azam, D. S. Rawat, *ChemMedChem* **2014**, *9*, 2439.
- [20] Y. Miyamoto, J. Kalisiak, K. Korthals, T. Lauwaet, D. Y. Cheung, R. Lozano, E. R. Cobo, P. Upcroft, J. A. Upcroft, D. E. Berg, F. D. Gillin, V. V. Fokin, K. B. Sharpless, L. Eckmann, *Proc. Natl. Acad. Sci. U. S. A.* **2013**, *110*, 17564.
- [21] A. M. Jarrad, T. Karoli, A. Debnath, C. Y. Tay, J. X. Huang, G. Kaeslin, A. G. Elliott, Y. Miyamoto, S. Ramu, A. M. Kavanagh, J. Zuegg, L. Eckmann, M. A. T. Blaskovich, M. A. Cooper, *Eur. J. Med. Chem.* **2015**, *101*, 96.
- [22] A. P. Wight, M. E. Davis, *Chem. Rev.* **2002**, *102*, 3589.
- [23] U. Díaz, M. Boronat, A. Corma, *Proc. R. Soc. a.* **2012**, *468*, 1927.
- [24] E. L. Margelefsky, R. K. Zeidan, M. E. Davis, *Chem. Soc. Rev.* **2008**, *37*, 1118.
- [25] R. K. Sharma, S. Sharma, S. Dutta, R. Zboril, M. B. Gawande, *Green Chem.* **2015**, *17*, 3207.
- [26] K. Lal, P. Rani, *ARKIVOC* **2016**, (i), 307.
- [27] P. Siemsen, R. C. Livingston, F. Diederich, *Angew. Chem. Int. Ed.* **2000**, *39*, 2632.
- [28] B. Gerard, J. Ryan, A. B. Beeler, J. A. Porco Jr., *Tetrahedron* **2006**, *62*, 6405.
- [29] T. Miao, L. Wang, *Synthesis* **2008**, *3*, 363.
- [30] M. N. Soltani Rad, S. Behrouz, M. M. Doroodmand, A. Movahedian, *Tetrahedron* **2012**, *68*, 7812.
- [31] M. N. Soltani Rad, S. Behrouz, S. J. Hoseini, H. Nasrabadi, M. Saberi Zare, *Helv. Chim. Acta* **2015**, *98*, 1210.
- [32] M. N. Soltani Rad, S. Behrouz, A. Movahedian, M. M. Doroodmand, Y. Ghasemi, S. Rasoul-Amini, A.-R. Ahmadi Gandomania, R. Rezaie, *Helv. Chim. Acta* **2013**, *96*, 688.
- [33] G. Pacchioni, L. Skuja and D. Griscom, *Defects in SiO₂ and Related Dielectrics: Science and Technology*, Springer, Dordrecht, Netherlands, **2000**, Vol. 2.
- [34] H. Firouzabadi, N. Iranpoor, B. Karimi, H. Hazarkhani, *Synlett* **2000**, *2000*, 263.
- [35] B. Xue, P. Chen, Q. Hong, J. Lin, K. L. Tan, *J. Mater. Chem.* **2001**, *11*, 2378.
- [36] E. Pahontu, V. Fala, A. Gulea, D. Poirier, V. Tapcov, T. Rosu, *Molecules* **2013**, *18*, 8812.
- [37] Q. Zhang, H. Ren, G. L. Baker, *Beilstein J. Org. Chem.* **2014**, *10*, 1365.
- [38] Z. Z. Liu, H. C. Chen, S. L. Cao, R. T. Li, *Synth. Commun.* **1993**, *23*, 2611.
- [39] M. W. Miller, US Patent, No: 3,479,367, **1969**.
- [40] M. N. Soltani Rad, S. Behrouz, M. Behrouz, A. Sami, M. Mardkhoshnood, A. Zarenezhad, E. Zarenezhad, *Mol. Diversity* **2016**, *20*, 705.
- [41] K. J. Esch, C. A. Petersen, *Clin. Microbiol. Rev.* **2013**, *26*, 58.
- [42] D. Leitsch, *Curr. Trop. Med. Rep.* **2015**, *2*, 128.

SUPPORTING INFORMATION

Additional supporting information may be found online in the Supporting Information section at the end of the article.

How to cite this article: Soltani Rad MN, Behrouz S, Mohammadtaghi-Nezhad J, Zarenezhad E, Agholi M. Silica-tethered cuprous acetophenone thiosemicarbazone (STCATSC) as a novel hybrid nano-catalyst for highly efficient synthesis of new 1,2,3-triazolyl-based metronidazole hybrid analogues having potent anti-giardial activity. *Appl Organometal Chem.* 2019; e4799. <https://doi.org/10.1002/aoc.4799>